

Effect of Chemical Treatment Sequence on Pineapple Peel Fiber: Chemical Composition, Thermal Stability and Thermal Degradation Kinetics

Paulo Henrique Fernandes Pereira (✉ femandes_eng@yahoo.com.br)

UNESP FEG: Universidade Estadual Paulista Julio de Mesquita Filho Faculdade de Engenharia -
Campus de Guaratingueta <https://orcid.org/0000-0002-9741-2161>

Heitor Luiz Ormaghi

Universidade Federal da Integracao Latino-Americana

Daniel Magalhães de Oliveira

UNESP FEG: Universidade Estadual Paulista Julio de Mesquita Filho Faculdade de Engenharia -
Campus de Guaratingueta

Barbara Pereira

USP EEL: Universidade de Sao Paulo Escola de Engenharia de Lorena

Valdeir Arantes

USP EEL: Universidade de Sao Paulo Escola de Engenharia de Lorena

Maria Odila Hilário Cioffi

UNESP FEG: Universidade Estadual Paulista Julio de Mesquita Filho Faculdade de Engenharia -
Campus de Guaratingueta

Research Article

Keywords: Fresh pineapple peel fibers, kinetic study, chemical treatment

Posted Date: January 13th, 2022

DOI: <https://doi.org/10.21203/rs.3.rs-1121648/v1>

License:  This work is licensed under a Creative Commons Attribution 4.0 International License.

[Read Full License](#)

Abstract

Millions of tons of fruit wastes are generated globally every year from residual agriculture, which makes essential to find alternative uses to increase their aggregate value and reduce the impact of environmental damage. The present study aimed to explore pineapple peel as an alternative source of cellulose by evaluating its composition and physical properties, which are essential to provide a clue to its application function diverse. Cellulose was extracted by a sequence of chlorine-free treatments to delignify the fresh pineapple peels, followed by characterization using chemical composition, XRD, FTIR, SEM and TGA to determine its crystallinity, structural properties, morphology thermal characteristics, and thermal degradation kinetic study. The result revealed that the pineapple peel amorphous segments containing hemicelluloses and lignin were extensively removed with increasing chemical treatments, leading to increased purity, crystallinity index and thermal stability of the extracted materials. The maximum degradation, and crystallinity index of the 2B isolated from the PPF are 150 °C and 80.91% respectively. The cellulose content increased from 24.05% (pineapple peel) to 80.91% (bleached cellulose). These results indicated that pretreatment via bleaching has suitable potential applications in nanocrystal production and suggests possible uses in the development of cellulose nanocrystal and application for packaging films.

1. Introduction

Increasing attention has been devoted to sustainability for moving towards eco-friendly products (Sabarinathan et al. 2020). Agroindustrial residues represent one of the most promising alternatives due to their remarkable characteristics such as low cost, biodegradability, abundance, ease of handling, and availability, besides being a renewable resource (Vinod et al. 2020; Halder and Purkait 2020; Debnath et al. 2021). In addition, agricultural residues like fruits and vegetables have been attracting attention from researchers and industries due to their potential to be converted into higher value bioproduct and to enhance the social and environmental benefits (Wang and Zhao 2021). However, about 40–50% of waste of root crops, fruits, and vegetables produced worldwide is discarded (Salehi and Aghajanzadeh 2020).

According to Oculi et al. 2020, pineapple (*Ananas comosus* (L) Merr.) is ranked the third most important tropical fruit crop worldwide after banana and citrus. As recently reported by the Food and Agriculture Organization (FAO), about 26 million pineapple tons were produced globally in 2019 (Hadidi et al. 2020). Brazil is the third pineapple producer worldwide, with plantations distributed throughout the territory and an estimated production of 2650.48 metric tons, behind the Philippines with 2671.71 metric tons and Costa Rica with 3056.45 metric tons produced in 2018 (Statista 2020). In the industry, pineapples are used for the manufacture of juices, jam, pulp, and syrup (Wu and Shiau 2015; Braga et al. 2020), with 20% of the whole pineapple fruit used for juice (Aruna 2019). However, about 35% of the total fresh pineapple weight is discarded (Dai and Huang 2017) after fruit processing (Kumar et al. 2021). A small portion of this residue may be used as livestock feed and fertilizer (Ketnawa et al. 2012), but most of it is burned as waste, resulting in environmental such as air pollution from smoke and haze (Gnanasekaran et

al. 2021). Thus, pineapple peel is an abundantly available potential source of cellulose that has been investigated for applications such as bioethanol production (Casabar et al. 2020), hydrogel (Dai et al. 2020), plasticizer (Rodsamran and Sothornvit 2019), adsorption (Shakya and Agarwal 2019), nanocellulose (Dai et al. 2019) and plasticizer (Rodsamran and Sothornvit 2019).

Many studies have been reported in the literature regarding pretreatments of agricultural residues for different purposes (Marques et al. 2020; Putrino et al. 2020; Contreras-Zarazúa et al. 2021; Yu et al. 2021). Specifically, alkaline hydrolysis is usually made using diluted or concentrated NaOH solution at low or high temperature (Bandyopadhyay-Ghosh et al., 2015, Cavali et al., 2020; Fonseca et al., 2019). In the presence of NaOH, the intramolecular ester bonds between lignin and hemicellulose are saponified, resulting in the extraction of lignin (Kim et al. 2016). Potassium hydroxide (KOH) is also used in alkali pretreatment for different feedstocks (Xie et al. 2018) to remove the remaining hemicellulose content (Bhagia et al. 2018). After the pretreatment, a second stage is necessary to remove various chromophore groups (from lignin) and impurities present in the cellulose fibers. There are different types of pretreatment found in the literature (Hongrattanavichit and Aht-Ong 2020); Flores-Velázquez et al., 2020; Vasco-Correa et al., 2019; Liu et al., 2019) with the primary goal of reducing the biomass in size and open its physical structure. In recent years, there is increasing use of H_2O_2 as a total or partial substitute for chlorine-based bleaching agents with elemental chlorine-free and totally chlorine-free sequences because of the compound's adverse environmental effects (Khristova et al. 2002).

Few studies have reported the effect of the pretreatment on the thermal kinetic behavior after cellulose separation using an eco-friendly treatment chemical. Therefore, the aim of this study is to understand the influence of pretreatments: alkaline treatment (NaOH 4% m/m) followed by a bleaching stage with H_2O_2 /NaOH, from pineapple peel on the physicochemical properties of its products separated as cellulose and to provide basic data for the utilization of biomass. To study the kinetic parameters, such as activation energy (E_a), thermogravimetric analysis (TGA) is used. The materials were characterized by scanning electron microscopy (SEM), chemical composition, thermogravimetric analysis (TGA), X-ray diffraction (XRD), Fourier transformed infrared spectroscopy (ATR-FTIR), and other means to provide a theoretical basis for the mechanism of kinetic studied

2. Material And Methods

2.1 Reagents

The chemicals used in this work were sodium hydroxide 97% w/w (NaOH), hydrogen peroxide 30% w/w (H_2O_2) purchased from Dinâmica, and potassium hydroxide 97% w/w (KOH) purchased from Vetec. The reagents were used as received without further purification.

2.2 Material

Pineapple peel fiber (PPF) from *Ananas comosus* L. Merrill pineapple used in this work was ripe fruit residue collected at a street market at Guaratinguetá city (São Paulo State, Brazil). Fresh PPF was

cleaned with tap water, cut into small pieces, and oven-dried at 60 °C for 48 h to remove all the moisture. Then, the PPFs were chopped into sizes of 2-4 cm in a cutter (GP 1500 AB) and milled to a powder (size less than 35 mesh) using a primary knife grinder (WILLYE TE-650).

2.3 Chemical treatments

2.3.1 Alkaline treatment (AT)

Briefly, 15 g of dried PPF was suspended with 900 mL of an aqueous NaOH 4% (w/v) at 70 °C for 1 h in ratio to solvent of 1:20, at 500 rpm in 2000 mL beaker. After 1 h, the treated fibers were filtered using a Buchner Funnel with a 28 µm pore filter, and the solid fraction was washed with distilled water until pH ~7 and oven-dried at 60 °C for 24 h to obtain the alkaline treated (AT) fibers.

2.3.2 First bleaching with H₂O₂ 30% (v/v)/NaOH 4% (w/v) (1B)

10g ried AT fiber was added in 600 mL of an aqueous NaOH solution (4% w/v) and 60 mL of H₂O₂ (30% v/v) at 70 °C, under mechanical stirring at 4000 rpm. After 1 h of reaction, 100 mL of NaOH (4% w/v) and 60 mL of H₂O₂ (30% v/v) were added into the reaction mixture. The same procedure was repeated each hour, up to 3 h. At the end of the 3 h, the fibers were vacuum filtered using a 28 µm pore filter and water-rinsed, washed with distilled water until pH ~7, and oven-dried at 60 °C for 24 h.

2.3.3 Second bleaching H₂O₂ 30% (v/v)/NaOH 4% (m/v) (2B)

Fibers from the 1B treatment were stirred in a solution of 600 mL NaOH (4% w/v) and 60 mL of H₂O₂ (30% v/v) at 70 °C, under mechanical stirring at 4000 rpm. The same procedure was repeated as described in item 2.3.2, except that the reaction was carried out for 2 h of reaction, hereafter referred to as 2B.

2.4 Characterization

2.4.1 Chemical composition

All samples were determined in triplicate. Fresh pineapple peel, AT, 1B, and 2B A were chemically analyzed following the NREL protocol (National Renewable Energy Laboratory) (Sluiter et al. 2012) to determine the percentages of lignin (soluble and insoluble), hemicellulose, and extractives in the fibers before and after each chemical treatment. Monomeric sugars were quantified by HPLC (Waters using an HPX-87H column (Bio-Rad)) at 45 °C and eluted with 5 mmol/L H₂SO₄ at 0.6 mL/min. Acid-soluble lignin content was determined at 205 nm, considering a molar absorptivity constant of 105 L/g.cm (Dence 1992). Soluble lignin content was determined following the protocol described in Dence (Dence 1992). Moisture, extractives, and ash contents were determined according to TAPPI T204 cm-97 (Technical Association of Pulp and Paper Industry 1997) and TAPPI T211 (Method and The 1993) protocols, respectively.

2.4.2 Fourier transformed infrared spectroscopy (FTIR)

FTIR analyses were carried out on the fresh pineapple peel, AT, 1B, and 2B to evaluate the samples functional groups. The FTIR spectra were determined using a Perkin Elmer spectrophotometer (Spectrum 100 model), operated with an attenuated total reflection (ATR) and in the transmittance method. Values were measured from 650 to 4000 cm^{-1} range with 12 scans.

2.4.3 X-ray diffraction (XRD)

The diffraction pattern of the fresh pineapple peel, AT, 1B, and 2Bs were analyzed by X-ray diffraction (XRD, SHIMADZU, Model XDR 6000) with a scanning radiation at 30 kV and 15 mA. All samples dried at 30 °C were scanned from a 2θ of 0° to 60°, with scan speed 0,001-0,002 min^{-1} . The crystallinity index (CrI) of the samples was calculated using the diffraction intensities of the crystalline structure and that of the amorphous fraction according to Segal's method. (L. Segal et al. 1959)

$$\text{CrI}\% = \frac{I(002) - I(\text{am})}{I(002)} \times 100$$

Where: $I(002)$ is the intensity of the crystalline peak at the maximum at 2θ between 22° and 23° for cellulose I, and $I(\text{am})$ is the intensity at the minimum at 2θ between 18° and 19° for cellulose I.

2.4.4 Thermal behavior

The thermal behavior of the PPF, AT, 1B and 2B fibers were analyzed on SII Nanotechnology INC equipment (Exstar 6000 model, TG/DTA 6200 series), operating under 100 mL/min constant nitrogen flow, in a temperature range of 30 to 750 °C and a 10 °C/min heating rate, and ~ 10 mg of oven-dried samples. For kinetic calculation, three additional heating rates (5, 20, and 40 °C. min^{-1}) were included. The kinetic study was carried out using a free Software (Kinetic Calculation v. 1.0 program) and considering Vyazovkin and Flynn-Wall-Ozawa methods (Drozin et al. 2020). The program Kinetic Calculations makes it possible to calculate kinetic substance decomposition parameters for thermogravimetric analysis through the Vyazovkin and the Ozawa–Flynn–Wall methods. More details in the kinetic calculation can be found on (Drozin et al. 2020). Only the activation energy values will be considered in this study for comparison among the samples.

2.5 Scanning electron microscopy (SEM)

The morphology of all the fibers were characterized by scanning electron microscopy (SEM) using a JEOL JSM 5319 equipment, with tungsten filament operating at 20kV, secondary electron detector, working at a distance of 15 mm and employing a low-vacuum technique. All fiber samples were coated with gold before SEM analysis.

3. Results And Discussion

3.1 Morphology and chemical composition

Fig. 1 displays the macroscopic visual images of pineapple peel fibers (PPF) after each chemical treatment (AT, 1B, and 2B). The dark brown color of the PPF changed into light brown after the alkaline treatment (AT).

After the first bleaching step (1B), a yellowish-white color is found, and after the second bleaching step (2B), a completely white color is noted. The variation in the color of PPF with the chemical treatments reflects the changes in chemical composition, with the removal of non-cellulosic materials such as lignin, hemicellulose, extractives, ashes, and oils. The same trend was observed in our previous studies (Cristina et al. 2020; Henrique et al. 2020b; Pereira et al. 2021).

The morphology of the fibers were investigated using SEM (Fig. 1a-m). Figure 1(a) shows that fresh pineapple peel had irregular morphologies with different particle sizes, massive wrinkled and depressed blocks (i.e., a kind of flakiness) as seen with a greater magnification (Fig.1b-c), a dense structure because non-cellulosic components such as pectin, lignin, and hemicellulose were intact. Similar morphologies structures have been reported by Zhang 2020 (Zhang et al. 2020). Meanwhile, AT resulted in fibers with a cleaner and smoother surface structure (Fig 1(d)). After AT, the cellulose fibers seem to be more exposed due to the removal of a percentage of amount of hemicellulose and lignin (Fig.1 e-f), as can be seen in the chemical analysis results as shown in Table 2. Hence, two subsequent treatment with step of bleaching to was necessary to remove these non-cellulosic materials in order to obtain a highly-pure cellulose.

Fig. 1(g) indicates that a homogeneous structure remained after 1B, which are shown by various agglomeration of macro fibrils with elongated walls (Fig. 1(h) and Fig. 1(i)). Finally, in Fig.1(j-m), a fibrous structure composed of microfibrils is easily noted with the fiber bundles and elongated rod forms.

The valorisation of pineapple waste into value-added products is influenced by its chemical composition. Table 1 displays the chemical composition of fresh pineapple peel with a comparison to others studies. The natural fibers are composed primarily of carbohydrate polymers (cellulose and hemicellulose), aromatic polymers (mainly lignin), and ashes. However, the composition of cellulose, hemicellulose, lignin, and ashes content of the pineapple peel might vary depending upon the season, variety, maturity period, and location of the cultivation of the pineapple (Banerjee et al. 2018). The fresh pineapple peel in the current study consisted of 24.1% cellulose, 29.3% hemicellulose, 6.3% lignin, and 5.0% ash.

Table 1. Chemical composition of fresh pineapple peel

Component (%)	Current Study	(Ban-Koffi and Han 1990)	(Casabar et al. 2020)	(Pardo et al. 2014)	(Rani and Nand 2004)
Cellulose	24.15 ±1.64	14.0	20.9	40.5	11.2
Hemicellulose	29.39 ±2.13	20.2	31.8	28.6	7.0
Lignin	6.35 ±0.28	1.5	10.4	10.1	11.2
Ash	5.05 ±0.10	0.6	9.9	1.5	3.8

After AT, the content cellulose increased to 65.2%, while hemicellulose (19.8%), lignin (3.1%), and ash (2.0%) decreased as expected (Table 2), indicating the effectiveness of sodium hydroxide treatment. For further removal of the non-cellulosic materials still remaining in the fiber after AT, these fibers were subjected to two alkaline bleaching steps (Table 2).

Table 2. Chemical composition of fresh pineapple peel (PPF), alkaline treatment (AT), 1B, and 2B

Component (%)	PPF	Alkaline treatment (AT)	1B	2B
Cellulose	24.15 ±1.64	65.22 ±4.6	77.94 ±4.79	80.72 ±5.15
Hemicellulose	29.39 ±2.13	19.86 ±2.39	15.88 ±0.32	12.09 ±0.28
Lignin	6.35 ±0.28	3.16 ±0.49	2.54 ±0.46	2.26 ±0.13
Ash	5.05 ±0.10	2.04 ±0.05	1.52 ±0.03	1.88 ±1.63
Extractives	32.8 ±0.63	*	*	*
Total	97.74 ±2.88	95.86 ±5.89	97.38 ± 5.42	100.73 ±4.83

*not analyzed

After the first bleaching (1B), the fiber still contained lignin and hemicellulose, indicating the need for another bleaching treatment. After the second bleaching step (2B), contents were 80.72% cellulose, 12.09% hemicellulose, and 2.26% lignin (Tabela 2). 2B fibers had a lower ash content (1.88%) than fresh pineapple peel (5.05%), indicating the presence of inorganic matter at a low content. The low ash content also indicates high pulp yield from pulping processes (Lopez et al. 2004). Pereira et al. (2021) found similar results for cellulose extraction from fresh pineapple crown (76.4% cellulose, 9.8% hemicellulose, and <1.1% lignin).

3.2 FTIR Analysis

FTIR was used to determine the main functional groups of pineapple peel fresh and the changes caused by the chemical treatments (Fig. 2). In the spectra, two common absorbance regions can be observed,

one from 750 to 1750 cm^{-1} and the other from 2250 to 3850 cm^{-1} . A similar pattern is observed for all samples. For example, no appearance/disappearance of bands is noted, but an increase in the polysaccharide group intensity ($\sim 1300\text{-}900 \text{ cm}^{-1}$) can be seen. The main bands appeared at 3330, 2900, 1730, 1640, 1512, 1200–1300, and 894 cm^{-1} .

The 3300 cm^{-1} and 2900 cm^{-1} bands correspond to the hydroxyl groups (inter, intra and free OH) (Dai and Fan 2011; Ornaghi et al. 2014) and to stretching vibration of methyl and methylene. The band at 1730 cm^{-1} is assigned to C=O in uronic acid. A similar pattern is observed among the samples, i.e., no appearance/disappearance of bands is noted, but an increase in the polysaccharide group intensity ($\sim 1300\text{-}900 \text{ cm}^{-1}$) can be seen. Also, a slight increase in the OH region intensity is observed for all treatments compared to the spectrum of the PPF. The PPF spectrum assigns some characteristic bands 1730, 1640, and 1512 cm^{-1} , also referred to hemicellulose and lignin. The 1730 cm^{-1} band peak is assigned to carbonyl stretching in unconjugated ketones and conjugated carbonyl groups (de Menezes Nogueira et al. 2019). It can be attributed either to the acetyl and uronic ester groups of hemicellulose or to the ester linkage of the carboxylic groups of ferulic and p-coumeric acids of lignin and/or hemicelluloses (Johari et al. 2016). The bands at 1512 cm^{-1} and 1640 cm^{-1} represent the aromatic C=C of lignin's aromatic rings (Hoareau et al. 2004). The band at 1253 cm^{-1} corresponds to C–O–C (aryl–alkyl ether) (Romanzini et al. 2013). This peak is generally observed when the guayacil ring, a subunit of the lignin macromolecule, is present (Li et al. 2020). All samples showed some characteristic signature bands of cellulose, including 3300, 2902, 1028, and 894 cm^{-1} , which corresponds to O-H stretching, C-H stretching, C-H deformation, C-O-C pyranose ring stretching vibration, and β -glycosidic linkages, respectively. As aforementioned, all these bands seem to slightly increase after the treatments (and maintaining a similar pattern) in comparison to PPF. The bands at 894 cm^{-1} for all samples are characteristic of β -glycosidic linkages between sugar molecules (Banerjee et al. 2019).

3.3 XRD Analysis

The diffractograms of each of the analysed samples (AT, 1B, and 2B) are present in Fig.3. The peaks at $2\theta=14.8^\circ$ and $2\theta=16.3^\circ$ corresponds to two overlapped weaker diffraction assigned of the (1-10) and (110) lattice planes (Besbes et al. 2011), a sharp peak at $2\theta=22.5^\circ$, which is assigned to the (200) lattice (French 2014a), and small and broad peak at $2\theta = 34.5^\circ$ represents the contribution of (040) plane (French 2014b; Tonoli et al. 2021). Only one peak ($2\theta = 22.5$) is observed in the reflective pattern of the fresh pineapple peel. This could be due to the presence of amorphous materials covering the crystalline portion of the fiber. After alkaline treatment and bleaching of the fresh pineapple, to obtain AT, 1B and 2B two new crystalline peaks emerged in the diffractogram of at $2\theta = 15.4^\circ$ and 34.5° . These peaks become more defined upon chemical treatments as expected. 2B, therefore, show 3 peaks at 15.4° , 22.5° and 34.5° similar to what has been reported for the (110), (200) and (004) crystallographic planes of cellulose I polymorph thus indicating that 2B has typical cellulose I structure (French and Santiago Cintrón 2013).

XRD analysis was conducted to provide the effect of the chemical treatments on the Segal empirical's crystallinity index (CrI.) (L.Segal et al. 1959). The CrI. was approximately 24.05, 53.74, 79.00, and 80.91% for PPF, AT, 1B, and 2B fibers, respectively. The crystallinity increased significantly from 24.05% to 80.91.8%. The higher crystallinity index of PPF compared to 1B (24.05 vs. 79%) could be well understood as a result of the removal of amorphous non-cellulosic compounds, induced by the purification treatment (alkali and bleaching treatments) performed to purify cellulose, which is due to the effective removal of amorphous components such as lignin, hemicellulose, waxes, and pectin with the treatments.

3.4 Thermogravimetric (TG) and thermal degradation kinetic

The TG and DTG curves of PPF before and after each chemical treatment (AT, 1B, and 2B) are shown in Fig (4a and 4b), with heating rate $10^{\circ}\text{Cmin}^{-1}$. The degradation temperatures for all samples can be observed in Table 3.

In general, the thermal decomposition of PPF can be divided into four main stages. The first stage corresponds to the temperature range of $30\text{-}140^{\circ}\text{C}$, and the mass loss is mainly attributed to moisture evaporation and low molecular mass components degradation (Pereira et al., 2020). This stage is observed for all samples, independently of the treatment. The other stages of mass loss are attributed to hemicellulose, cellulose, and lignin components. For the treated fibers, only one peak referred to as cellulose is observed, showing that the remained non-cellulosic components have a small influence on the degradation stages. All treated curves showed similar behavior. The second stage corresponds to the decomposition of hemicellulose and part of cellulose (cleavage of cellulose glycosidic bonds) (Hu et al. 2020; Marques et al. 2020). Finally, lignin degrades in a wide temperature range ($100\text{-}900^{\circ}\text{C}$) (Melikoğlu et al. 2019; Ornaghi et al. 2020).

For 1B and 2B fibers, the more pronounced mass loss was observed between 300 and 400°C . The major cellulosic chain degradation is due to several steps, such as depolymerization, dehydration, and decomposition of the glycosidic units (Gabriel et al. 2020). Also, the thermal stability of fibers bleached increases after each chemical treatment (Table 3).

Table 3. Degradation stages and main mass loss for the PPF before and after the chemical treatments. Data obtained for the heating rate at $10^{\circ}\text{C.min}^{-1}$

Sample	T _{onset} (°C)	Thermal event (°C)	Mass loss (%)	T _{peak} (°C)	Residue _{750 °C} (%)
PPF	126	126 – 223	16.4	198	30.2
		223 – 295	19.1	258	
		295 – 600	27.5	326	
AT	174	174 – 600	78.6	338	15.7
1B	180	180 – 600	80.2	346	15.5
2B	183	183 – 600	80.7	351	15.1

The activation energies were calculated using free available Software (Kinetic Calculation v. 1.0 program) (Drozin et al. 2020) and are presented in Figure 5. The conversion range (α) from 0.2 to 0.8 was used according to the recommendation in Drozin 2020 (Drozin et al. 2020) due to the inaccuracy of the process's mathematical description. Vyazovkin and FWO methods were used to estimate the E_a . In general, all treatments gave a more linear activation energy distribution than the PPF, which increases with conversion degree. The values obtained are presented in Table 4. A relative error higher than 10% indicates a multi-step mechanism degradation, which only occurs for PPF. In general, the linearity of distribution of activation energy can be attributed to the predominant presence of cellulose (indicating a single-step mechanism degradation), which increased by treatment due to removal of more impurities and non-cellulosic components, i.e., in this case, higher E_a was proportional to the crystallinity index with the exception of the PPF.

It is important to mention (and can be counterintuitive) that the higher crystallinity for the treated samples (as observed in XRD, morphology, and chemical composition) does not necessarily means higher activation energies due to the complex pyrolysis behavior of this type of materials. Hence, the higher crystallinity for lignocellulosic materials (mainly in our case) is indicative of a more homogeneous E_a distribution and not higher values per se.

Table 4. Activation energy values for Vyazovkin and FWO methods with the respective relative error for PPF before and after the chemical treatments

Samples	$E_{aVyazovkin}$ (KJ/mol)	E_{aFWO} (KJ/mol)	Relative error (%)
PPF	296.11	310.28	35.3
AT	168.17	184.87	3.4
1B	173.89	193.83	2.2
2B	175.52	195.58	2.7

4. Conclusions

In this study, cellulose fibers were successfully extracted from pineapple peels characterized in terms of physical, chemical, thermal, and morphological properties. The high cellulose content and low hemicellulose after the alkaline treatment sequence lead to cellulose, which has great potential applications in the automotive industry as reinforcement polymeric, and produce cellulose nanocrystal to use as food packaging material. Three-stage extraction was beneficial to maintain the morphology of cellulose fibers, which produced cellulose I with high purity and crystallinity (80.91 %). The alkaline treatment showed higher efficiency in removing the lignocellulosic compound, as it was confirmed via FTIR and compositional analyses. The kinetic parameters of the degradation of PPF, AT, 1B, and 2B were accurately determined from a series of TGA experiments at four heating rates. The E_a value of the degradation of the PPF calculated using Vyazovkin and Flynn-Wall-Ozawa methods based on TGA and DTGA curves are higher than those of AT, 1B, and 2B materials. The activation energy required for initiating the thermal degradation after alkaline treatment was less than the value calculated to 2B due to quantities de hemicellulose and lignin in the structure. The calculated average apparent activation energy value through Vyazovkin and FWO methods were 175.52 and 195.58 kJ mol^{-1} for bleached cellulose (2B), while to AT were 168.17 and 184.87 kJ mol^{-1} , respectively. From the above conclusion, it can say it's possible to conversion of fruit residue into a high-value product and generated new information about the specific treatment conditions, bleaching condition for obtaining high-quality cellulose, and environmentally friendly cellulose extraction methods for applications in diverse areas.

Declarations

Acknowledgments

This research was financially supported by the São Paulo Research Foundation (FAPESP, Brazil) Grant n° 2015/10386–9.

References

- Aruna TE (2019) Production of value-added product from pineapple peels using solid state fermentation. *Innov Food Sci Emerg Technol* 57:102193. <https://doi.org/10.1016/j.ifset.2019.102193>
- Ban-Koffi L, Han YW (1990) Alcohol production from pineapple waste. *World J Microbiol Biotechnol* 6:281–284. <https://doi.org/10.1007/BF01201297>
- Bandyopadhyay-Ghosh S, Ghosh SB, Sain M (2015) The use of biobased nanofibres in composites. In: *Biofiber Reinforcements in Composite Materials*. Elsevier, pp 571–647
- Banerjee S, Patti AF, Ranganathan V, Arora A (2019) Hemicellulose based biorefinery from pineapple peel waste: Xylan extraction and its conversion into xylooligosaccharides. *Food Bioprod Process* 117:38–50. <https://doi.org/10.1016/j.fbp.2019.06.012>
- Banerjee S, Ranganathan V, Patti A, Arora A (2018) Valorisation of pineapple wastes for food and therapeutic applications. *Trends Food Sci Technol* 82:60–70. <https://doi.org/https://doi.org/10.1016/j.tifs.2018.09.024>
- Besbes I, Alila S, Boufi S (2011) Nanofibrillated cellulose from TEMPO-oxidized eucalyptus fibres: Effect of the carboxyl content. *Carbohydr Polym* 84:975–983. <https://doi.org/10.1016/j.carbpol.2010.12.052>
- Bhagia S, Pu Y, Evans BR, et al (2018) Hemicellulose characterization of deuterated switchgrass. *Bioresour Technol* 269:567–570. <https://doi.org/10.1016/j.biortech.2018.08.034>
- Braga V, Guidi LR, de Santana RC, Zotarelli MF (2020) Production and characterization of pineapple-mint juice by spray drying. *Powder Technol* 375:409–419. <https://doi.org/10.1016/j.powtec.2020.08.012>
- Casabar JT, Ramaraj R, Tipnee S, Unpaprom Y (2020) Enhancement of hydrolysis with *Trichoderma harzianum* for bioethanol production of sonicated pineapple fruit peel. *Fuel* 279:118437. <https://doi.org/10.1016/j.fuel.2020.118437>
- Cavali M, Socol CR, Tavares D, et al (2020) Effect of sequential acid-alkaline treatment on physical and chemical characteristics of lignin and cellulose from pine (*Pinus* spp.) residual sawdust. *Bioresour Technol* 316:123884. <https://doi.org/10.1016/j.biortech.2020.123884>
- Contreras-Zarazúa G, Martin-Martin M, Sánchez-Ramírez E, Segovia-Hernández JG (2021) Furfural production from agricultural residues using different intensified separation and pretreatment alternatives. Economic and environmental assessment. *Chem Eng Process - Process Intensif* 108569. <https://doi.org/10.1016/j.cep.2021.108569>

- Cristina K, Carvalho C De, Heitor B, et al (2020) Survey on chemical , physical , and thermal prediction behaviors for sequential chemical treatments used to obtain cellulose from *Imperata Brasiliensis*. *J Therm Anal Calorim*. <https://doi.org/10.1007/s10973-019-09221-5>
- Dai D, Fan M (2011) Investigation of the dislocation of natural fibres by Fourier-transform infrared spectroscopy. *Vib Spectrosc* 55:300–306. <https://doi.org/10.1016/j.vibspec.2010.12.009>
- Dai H, Huang H (2017) Synthesis, characterization and properties of pineapple peel cellulose-g-acrylic acid hydrogel loaded with kaolin and sepia ink. *Cellulose* 24:69–84. <https://doi.org/10.1007/s10570-016-1101-0>
- Dai H, Huang Y, Zhang H, et al (2020) Direct fabrication of hierarchically processed pineapple peel hydrogels for efficient Congo red adsorption. *Carbohydr Polym* 230:115599. <https://doi.org/10.1016/j.carbpol.2019.115599>
- Dai H, Zhang H, Ma L, et al (2019) Green pH/magnetic sensitive hydrogels based on pineapple peel cellulose and polyvinyl alcohol: synthesis, characterization and naringin prolonged release. *Carbohydr Polym* 209:51–61. <https://doi.org/10.1016/j.carbpol.2019.01.014>
- de Menezes Nogueira I, Avelino F, de Oliveira DR, et al (2019) Organic solvent fractionation of acetosolv palm oil lignin: The role of its structure on the antioxidant activity. *Int J Biol Macromol* 122:1163–1172. <https://doi.org/10.1016/j.ijbiomac.2018.09.066>
- Debnath B, Haldar D, Purkait MK (2021) A critical review on the techniques used for the synthesis and applications of crystalline cellulose derived from agricultural wastes and forest residues. *Carbohydr Polym* 273:118537. <https://doi.org/10.1016/j.carbpol.2021.118537>
- Dence CW (1992) The Determination of Lignin. In: Lin SY, Dence CW (eds) *Methods in Lignin Chemistry*. Springer Berlin Heidelberg, Berlin, pp 33–61
- Drozin D, Sozykin S, Ivanova N, et al (2020) Kinetic calculation: Software tool for determining the kinetic parameters of the thermal decomposition process using the Vyazovkin Method. *SoftwareX* 11:100359. <https://doi.org/10.1016/j.softx.2019.100359>
- Fonseca AS, Panthapulakkal S, Konar SK, et al (2019) Improving cellulose nanofibrillation of non-wood fiber using alkaline and bleaching pre-treatments. *Ind Crops Prod* 131:203–212. <https://doi.org/10.1016/j.indcrop.2019.01.046>
- French AD (2014a) Idealized powder diffraction patterns for cellulose polymorphs. *Cellulose* 21:885–896. <https://doi.org/10.1007/s10570-013-0030-4>
- French AD (2014b) Idealized powder diffraction patterns for cellulose polymorphs. *Cellulose* 21:885–896. <https://doi.org/10.1007/s10570-013-0030-4>

- French AD, Santiago Cintrón M (2013) Cellulose polymorphy, crystallite size, and the Segal Crystallinity Index. *Cellulose* 20:583–588. <https://doi.org/10.1007/s10570-012-9833-y>
- Gabriel T, Belete A, Syrowatka F, et al (2020) Extraction and characterization of celluloses from various plant byproducts. *Int J Biol Macromol* 158:1248–1258. <https://doi.org/10.1016/j.ijbiomac.2020.04.264>
- Gnanasekaran S, Nordin NIAA, Jamari SS, Shariffuddin JH (2021) Effect of Steam-Alkaline coupled treatment on N36 cultivar pineapple leave fibre for isolation of cellulose. *Mater Today Proc.* <https://doi.org/10.1016/j.matpr.2021.02.216>
- Hadidi M, Amoli PI, Jelyani AZ, et al (2020) Polysaccharides from pineapple core as a canning by-product: Extraction optimization, chemical structure, antioxidant and functional properties. *Int J Biol Macromol* 163:2357–2364. <https://doi.org/10.1016/j.ijbiomac.2020.09.092>
- Haldar D, Purkait MK (2020) Micro and nanocrystalline cellulose derivatives of lignocellulosic biomass: A review on synthesis, applications and advancements. *Carbohydr Polym* 250:116937. <https://doi.org/10.1016/j.carbpol.2020.116937>
- Hoareau W, Trindade WG, Siegmund B, et al (2004) Sugar cane bagasse and curaua lignins oxidized by chlorine dioxide and reacted with furfuryl alcohol: characterization and stability. *Polym Degrad Stab* 86:567e576. <https://doi.org/10.1016/j.polymdegradstab.2004.07.005>
- Hongrattanavichit I, Aht-Ong D (2020) Nanofibrillation and characterization of sugarcane bagasse agro-waste using water-based steam explosion and high-pressure homogenization. *J Clean Prod* 277:123471. <https://doi.org/10.1016/j.jclepro.2020.123471>
- Hu L, Peng H, Xia Q, et al (2020) Effect of ionic liquid pretreatment on the physicochemical properties of hemicellulose from bamboo. *J Mol Struct* 1210:128067. <https://doi.org/10.1016/j.molstruc.2020.128067>
- Johari AP, Kurmvanshi SK, Mohanty S, Nayak SK (2016) Influence of surface modified cellulose microfibrils on the improved mechanical properties of poly (lactic acid). *Int J Biol Macromol* 84:329–339. <https://doi.org/10.1016/j.ijbiomac.2015.12.038>
- Ketnawa S, Chaiwut P, Rawdkuen S (2012) Pineapple wastes: A potential source for bromelain extraction. *Food Bioprod Process* 90:385–391. <https://doi.org/10.1016/j.fbp.2011.12.006>
- Khristova P, Tomkinson J, Valchev I, et al (2002) Totally chlorine-free bleaching of flax pulp. *Bioresour Technol* 85:79–85. [https://doi.org/10.1016/S0960-8524\(02\)00022-6](https://doi.org/10.1016/S0960-8524(02)00022-6)
- Kim JS, Lee YY, Kim TH (2016) A review on alkaline pretreatment technology for bioconversion of lignocellulosic biomass. *Bioresour Technol* 199:42–48. <https://doi.org/10.1016/j.biortech.2015.08.085>
- Kumar K, Srivastav S, Sharanagat VS (2021) Ultrasound assisted extraction (UAE) of bioactive compounds from fruit and vegetable processing by-products: A review. *Ultrason Sonochem* 70:105325.

<https://doi.org/10.1016/j.ultsonch.2020.105325>

Li J, Bai X, Fang Y, et al (2020) Comprehensive mechanism of initial stage for lignin pyrolysis. *Combust Flame* 215:1–9. <https://doi.org/10.1016/j.combustflame.2020.01.016>

Marques FP, Silva LMA, Lomonaco D, et al (2020) Steam explosion pretreatment to obtain eco-friendly building blocks from oil palm mesocarp fiber. *Ind Crops Prod* 143:111907. <https://doi.org/10.1016/j.indcrop.2019.111907>

Melikoğlu AY, Bilek SE, Cesur S (2019) Optimum alkaline treatment parameters for the extraction of cellulose and production of cellulose nanocrystals from apple pomace. *Carbohydr Polym* 215:330–337. <https://doi.org/10.1016/j.carbpol.2019.03.103>

Method O, The T (1993) Determination of equilibrium moisture in pulp , paper and paperboard for chemical analysis. 1–3

Oculi J, Bua B, Ocwa A (2020) Reactions of pineapple cultivars to pineapple heart rot disease in central Uganda. *Crop Prot* 135:105213. <https://doi.org/10.1016/j.cropro.2020.105213>

Ornaghi HL, Ornaghi FG, Neves RM, et al (2020) Mechanisms involved in thermal degradation of lignocellulosic fibers: a survey based on chemical composition. *Cellulose* 27:4949–4961. <https://doi.org/10.1007/s10570-020-03132-7>

Ornaghi HL, Poletto M, Zattera AJ, Amico SC (2014) Correlation of the thermal stability and the decomposition kinetics of six different vegetal fibers. *Cellulose* 21:177–188. <https://doi.org/10.1007/s10570-013-0094-1>

Pardo MES, Cassellis MER, Escobedo RM, García EJ (2014) Chemical Characterisation of the Industrial Residues of the Pineapple (*Ananas comosus*). *J Agric Chem Environ* 03:53–56. <https://doi.org/10.4236/jacen.2014.32b009>

Pereira PHF, Ornaghi HL, Arantes V, Cioffi MOH (2021) Effect of chemical treatment of pineapple crown fiber in the production, chemical composition, crystalline structure, thermal stability and thermal degradation kinetic properties of cellulosic materials. *Carbohydr Res* 499:108227. <https://doi.org/10.1016/j.carres.2020.108227>

Pereira, PHF, Luiz H, et al (2020) Obtaining cellulose nanocrystals from pineapple crown fibers by free-chlorite hydrolysis with sulfuric acid: physical , chemical and structural characterization. *Cellulose* 27:5745-5756. <http://dx.doi.org/10.1007/s10570-020-03179-6>

Pereira, PHF, Souza NF, et al (2020) Comparative analysis of different chlorine-free extraction on oil palm mesocarp fiber. *Industrial Crops & Products* 150: 112305. <https://doi.org/10.1016/j.indcrop.2020.112305>

- Pereira PHF, Voorwald HCJ, Cioffi MOH, et al (2011) Sugarcane bagasse pulping and bleaching: Thermal and chemical characterization. *BioResources* 6(3) 2471-2482.
- Putrino FM, Tedesco M, Bodini RB, Oliveira AL de (2020) Study of supercritical carbon dioxide pretreatment processes on green coconut fiber to enhance enzymatic hydrolysis of cellulose. *Bioresour Technol* 309:123387. <https://doi.org/10.1016/j.biortech.2020.123387>
- Rani DS, Nand K (2004) Ensilage of pineapple processing waste for methane generation. *Waste Manag* 24:523–528. <https://doi.org/10.1016/j.wasman.2003.10.010>
- Rodsamran P, Sothornvit R (2019) Preparation and characterization of pectin fraction from pineapple peel as a natural plasticizer and material for biopolymer film. *Food Bioprod Process* 118:198–206. <https://doi.org/10.1016/j.fbp.2019.09.010>
- Romanzini D, Lavoratti A, Ornaghi HL, et al (2013) Influence of fiber content on the mechanical and dynamic mechanical properties of glass / ramie polymer composites. *Mater Des* 47:9–15. <https://doi.org/10.1016/j.matdes.2012.12.029>
- Sabarinathan P, Rajkumar K, Annamalai VE, Vishal K (2020) Characterization on chemical and mechanical properties of silane treated fish tail palm fibres. *Int J Biol Macromol* 163:2457–2464. <https://doi.org/10.1016/j.ijbiomac.2020.09.159>
- Salehi F, Aghajanzadeh S (2020) Effect of dried fruits and vegetables powder on cakes quality: A review. *Trends Food Sci Technol* 95:162–172. <https://doi.org/10.1016/j.tifs.2019.11.011>
- Segal L, Creely JJ, Martin AE, Conrad CM (1959b) An Empirical Method for Estimating the Degree of Crystallinity of Native Cellulose Using the X-Ray Diffractometer. *Text Res J* 29:786–794. <https://doi.org/10.1177/004051755902901003>
- Shakya A, Agarwal T (2019) Removal of Cr(VI) from water using pineapple peel derived biochars: Adsorption potential and re-usability assessment. *J Mol Liq* 293:111497. <https://doi.org/10.1016/j.molliq.2019.111497>
- Sluiter a., Hames B, Ruiz R, et al (2012) NREL/TP-510-42618 analytical procedure - Determination of structural carbohydrates and lignin in Biomass. *Lab Anal Proced* 17. <https://doi.org/NREL/TP-510-42618>
- Statista (2020) No Title. In: Lead. Ctries. pineapple Prod. worldwide 2017. <https://www.statista.com/statistics/298517/global-pineapple-production-by-leading-countries/>.
- Technical Association of Pulp and Paper Industry (1997) T204 cm-97. Solvent extractives of wood and pulp. *TAPPI test methods* 12. <https://doi.org/10.5772/916>
- Tonoli GHD, Holtman K, Silva LE, et al (2021) Changes on structural characteristics of cellulose pulp fiber incubated for different times in anaerobic digestate. *CERNE* 27:.

<https://doi.org/10.1590/01047760202127012647>

Vinod A, Sanjay MR, Suchart S, Jyotishkumar P (2020) Renewable and sustainable biobased materials: An assessment on biofibers, biofilms, biopolymers and biocomposites. *J Clean Prod* 258:120978.

<https://doi.org/10.1016/j.jclepro.2020.120978>

Wang T, Zhao Y (2021) Optimization of bleaching process for cellulose extraction from apple and kale pomace and evaluation of their potentials as film forming materials. *Carbohydr Polym* 253:117225.

<https://doi.org/10.1016/j.carbpol.2020.117225>

Wu M-Y, Shiau S-Y (2015) Effect of the Amount and Particle Size of Pineapple Peel Fiber on Dough Rheology and Steamed Bread Quality. *J Food Process Preserv* 39:549–558.

<https://doi.org/10.1111/jfpp.12260>

Xie X, Feng X, Chi S, et al (2018) A sustainable and effective potassium hydroxide pretreatment of wheat straw for the production of fermentable sugars. *Bioresour Technol Reports* 3:169–176.

<https://doi.org/10.1016/j.biteb.2018.07.014>

Yu Y, Lau A, Sokhansanj S (2021) Improvement of the pellet quality and fuel characteristics of agricultural residues through mild hydrothermal treatment. *Ind Crops Prod* 169:113654.

<https://doi.org/10.1016/j.indcrop.2021.113654>

Zhang L, Yang Z, Li S, et al (2020) Comparative study on the two-step pyrolysis of different lignocellulosic biomass: Effects of components. *J Anal Appl Pyrolysis* 104966.

<https://doi.org/10.1016/j.jaap.2020.104966>

Figures

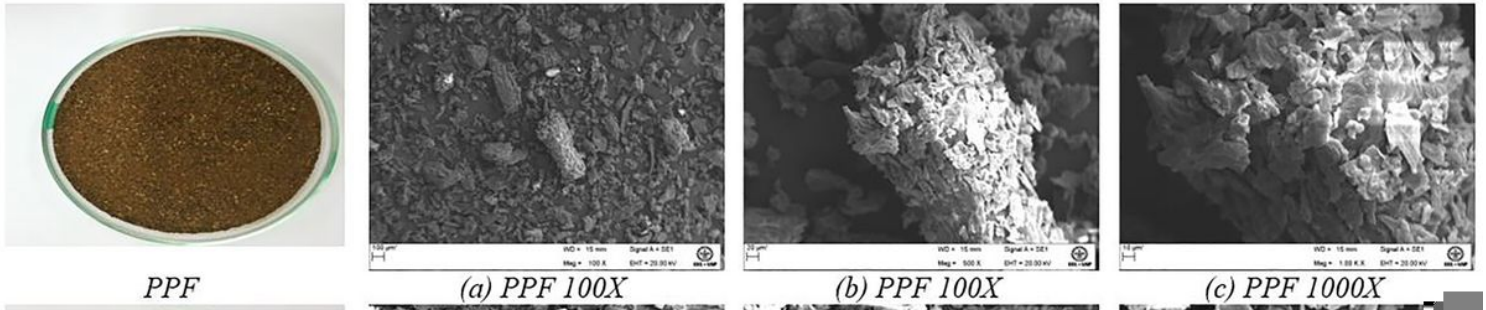


Figure 1

Visual aspect and SEM images of fresh pineapple peel (PPF) and treated samples (AT, 1B, and 2B)

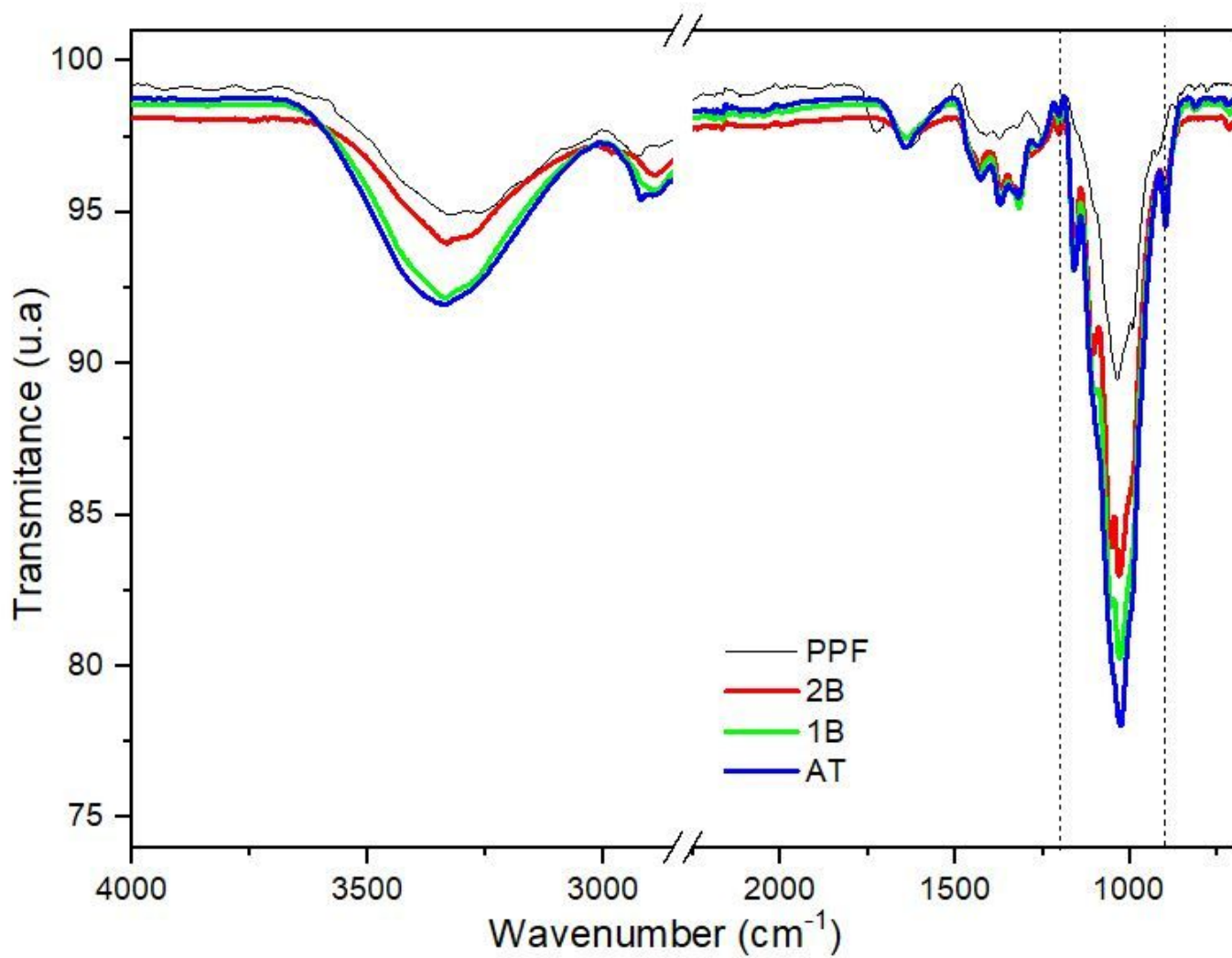


Figure 2

FTIR of fresh pineapple peel (PPF) and treated samples (AT, 1B, and 2B)

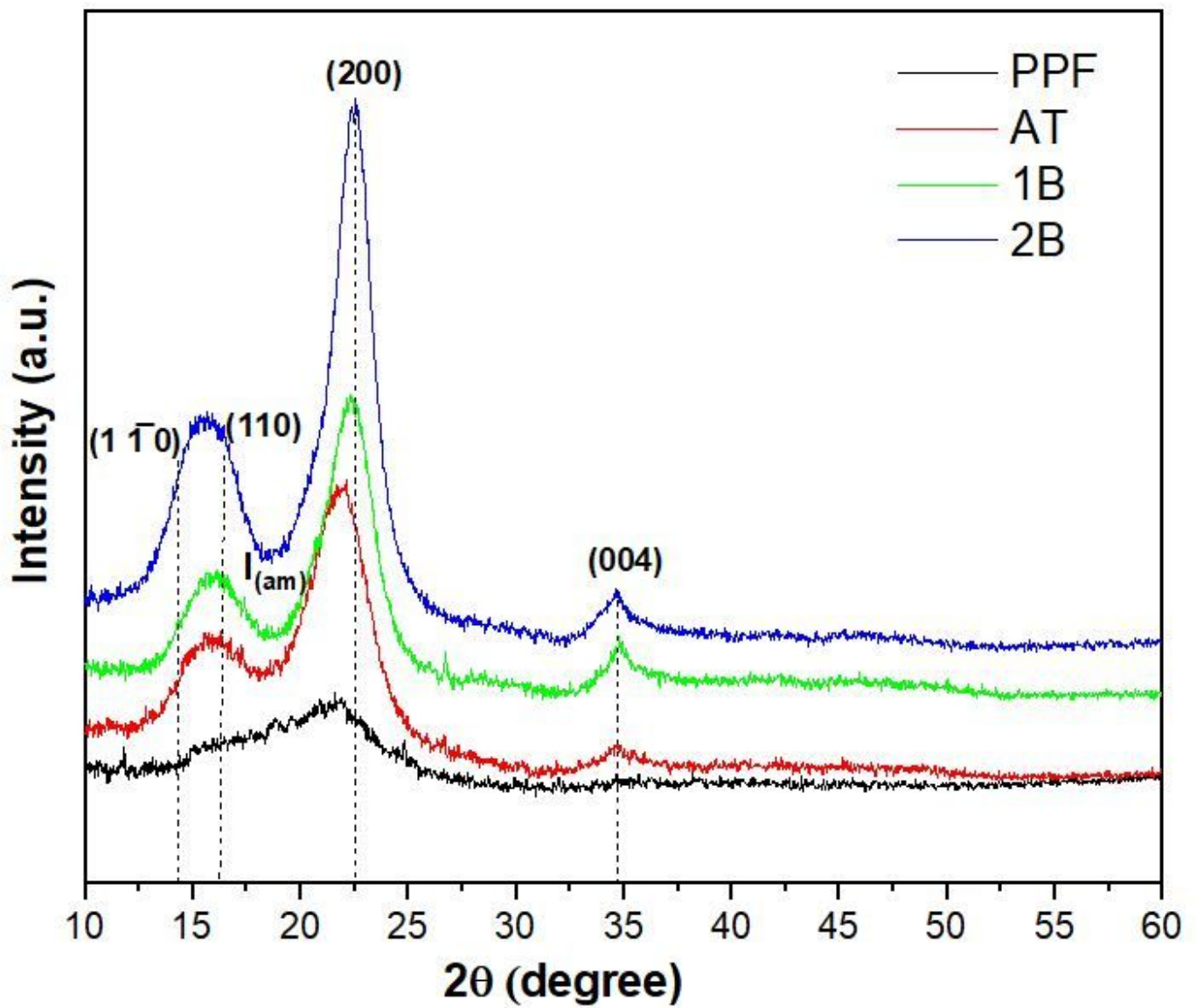


Figure 3

XRD pattern for PPF, AT, 1B, and 2B fibers. The dotted lines are a guide for the eyes

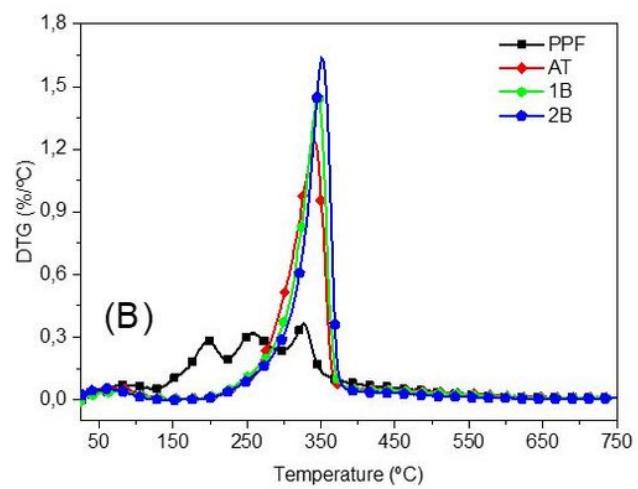
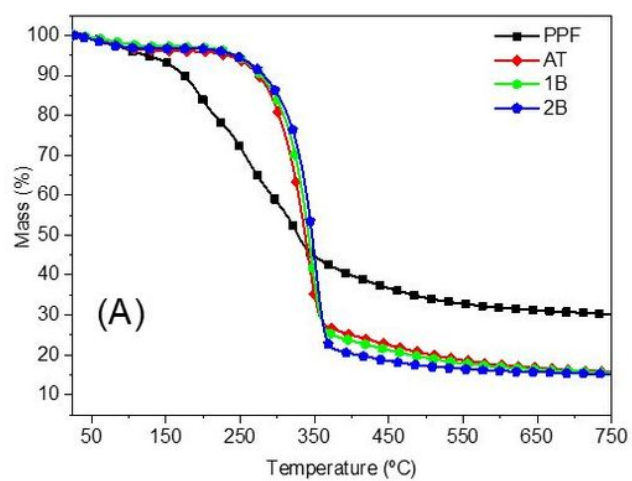


Figure 4

(A) TG and (B) DTG of PPF and treated samples (AT, 1B, 2B)

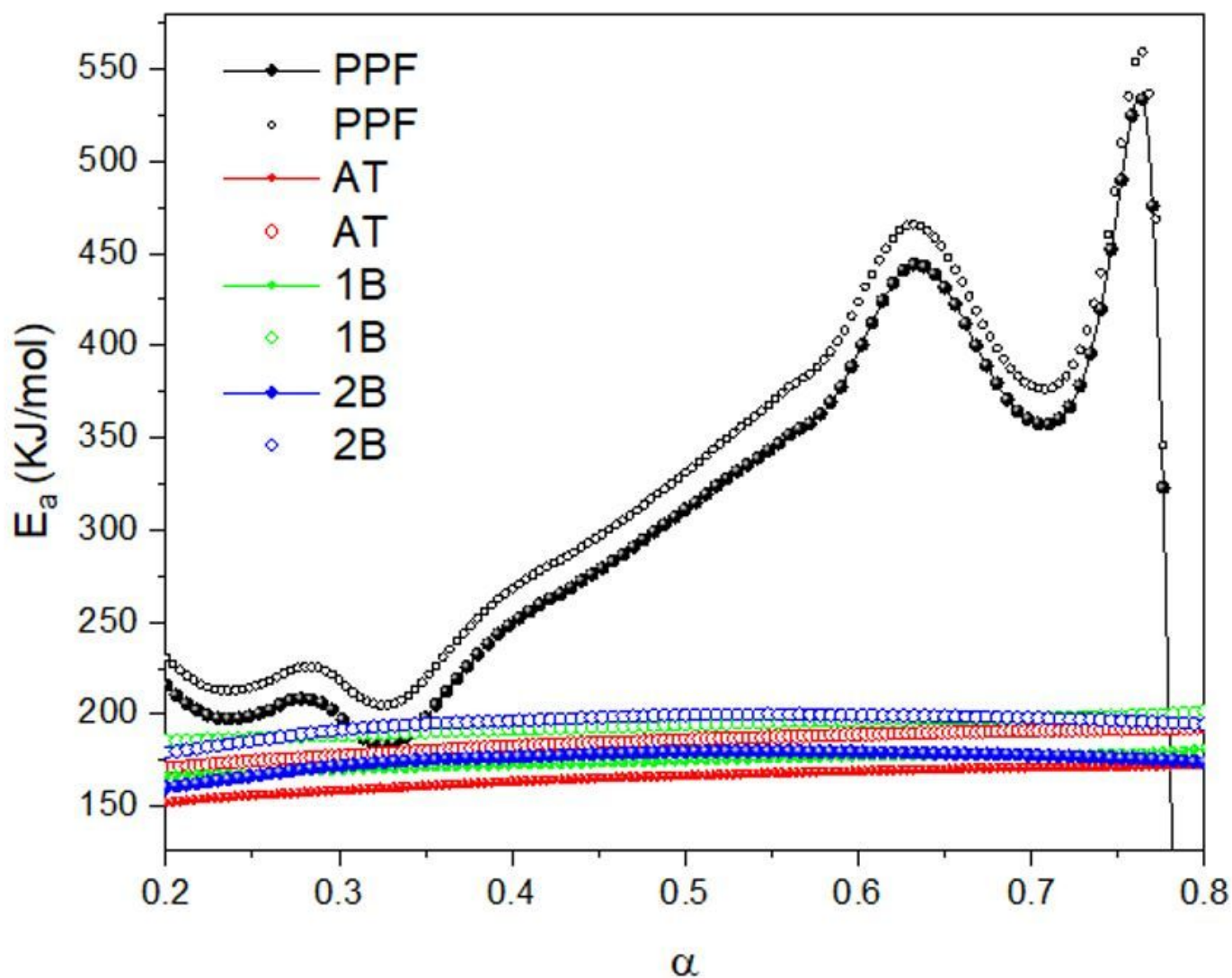


Figure 5

Vyazovkin and FWO activation energies calculated for PPF before and after the chemical treatments. The solid lines represent the fit for Vyazovkin method while the empty circles are the FWO ones.

Supplementary Files

This is a list of supplementary files associated with this preprint. Click to download.

- [GraphicAbstract.docx](#)
- [ManuscriptRef.Cels.D212101298R21.docx](#)